Sapena-Bano, A.; Manuel Pineda-Sanchez; Rubén Puche-Panadero; Martinez-Roman, J.; Matic, D. (2015). Fault Diagnosis of Rotating Electrical Machines in Transient Regime Using a Single Stator Current's FFT. IEEE Transactions on Instrumentation and Measurement. 64(11):3137-3146. doi:10.1109/TIM.2015.2444240

Fault Diagnosis of Rotating Electrical Machines in Transient Regime Using a Single Stator Current's FFT

A. Sapena-Baño, M. Pineda-Sanchez, *Member, IEEE*, R. Puche-Panadero, *Member, IEEE*, J. Martinez-Roman, and D. Matić, *Member, IEEE*.

***Abstract*—The discrete wavelet transform has attracted a rising interest in recent years to monitor the condition of rotating electrical machines in transient regime, because it can reveal the time-frequency behaviour of the current's components associated to fault conditions. Nevertheless, the implementation of the wavelet transform, especially on embedded or low-power devices, faces practical problems, such as the election of the mother wavelet, the tuning of its parameters, the coordination between the sampling frequency and the levels of the transform, and the construction of the bank of wavelet filters, with highly different bandwidths, that constitute the core of the discrete wavelet transform. In this paper, a diagnostic system using the harmonic wavelet transform is proposed, which can alleviate these practical problems because it is built using a single FFT of one phase's current. The harmonic wavelet was conceived to perform musical analysis, hence its name, and it has spread into many fields, but, up to the best of the authors' knowledge, it has not been applied before to perform fault diagnosis of rotating electrical machines in transient regime using the stator current. The simplicity and performance of the proposed approach are assessed by comparison with other types of wavelet transforms, and it has been validated with the experimental diagnosis of a 3.15 MW induction motor with broken bars.**

***Index Terms*—Harmonic wavelet, Discrete wavelet transform, Discrete wavelet packet transform, Condition monitoring, Fault diagnosis, Fourier transforms, Signal processing.**

I. Introduction

FAULT diagnosis of rotating electrical machines through the analysis of the machine's current signature (MCSA) is a widely spread diagnostic method, whose rapid expansion can be explained, albeit partially, by the simplicity of its implementation. On the hardware side, it requires just a single current's clamp or sensor, so it can be applied online without disturbing the normal machine's operation. On the software side, a simple FFT is needed to generate the power spectrum of the current in the search for characteristic fault harmonics. However, at the same time, the use of the power spectrum restricts the application of MCSA to machines working in steady state [1]. In effect, in the case of time varying conditions, such as oscillating loads, motors fed from variable speed drives (VSD) with continuous changes of speed, wind generators, or even during the start-up transient, the power spectrum of the current does not display any sharp peak at the frequencies associated to the machine's faults. Instead, a wide area is filled by the fault harmonics as their frequency varies with the speed, the slip or the supply's frequency [2]. Anyway, this inability of MCSA to operate correctly in transient regime is not a limitation of the FFT itself, but of the use for diagnostic purposes of the modulus of the FFT of the current, or its squared value. In fact, any arbitrary signal, as the motor current in transient regime, can be fully described either in the time domain, or in the frequency domain (using its complex spectrum, that is, both the modulus and the argument of its Fourier transform), and it can be converted from one domain to the other one without any loss or distortion.

To overcome the limitations of MCSA in transient condition, new techniques have been developed to track the fault harmonics, even if they are non-stationary, using advanced transforms that are able to display the evolution of the fault harmonics in the time-frequency domain [3], [4]. The short time Fourier transform (STFT) is a natural extension of the FFT, by repetitively performing the FFT of the current signal multiplied by a short, time-sliding window [5], [6]. During the length of this window, the current can be considered to be a nearly steady signal, so that its spectrum gives a meaningful display of the frequency content of the current at the central time of the window. But the effect of multiplying the signal by a time window has the effect of convolving the frequency transforms of the signal and the window, so an improvement on the time resolution implies a reduction of the frequency resolution, as the Heisenberg's principle states, and vice versa. This implies that to display correctly harmonics components with a low frequency variation, long time windows must be used, while the analysis of components with a high frequency variation requires the use of short time windows. If the current signal contains both type of components, a trade-off between good time resolution and good frequency resolution must be made. A solution to this problem is the use of a multi-resolution transform, such as the wavelet transform (WT) [7], which uses simultaneously long time windows to extract the low frequency components of the signal, and short time windows to correctly locate in the time axis the high frequency components of the signal. To do so, the WT uses a single

This work was supported by the Spanish "Ministerio de Ciencia e Innovación" in the framework of the "Programa Nacional de proyectos de Investigación Fundamental" (project reference DPI2011-23740).

A. Sapena-Baño (sapena.angel@gmail.com), M. Pineda-Sanchez (mpineda@die.upv.es), R. Puche-Panadero (rupucpa@die.upv.es), and J. Martinez-Roman (jmroman@die.upv.es) are with the Department of Electrical Engineering, Universitat Politècnica de València, Camino de Vera s/n, 46022, Valencia, Spain. D. Matić (dmatic@uns.ac.rs) is with the Department of Computing and Control Department, University of Novi Sad, Serbia.

mother wavelet that is shifted in the time domain and scaled in the frequency domain, giving variable shaped Heisenberg boxes, with constant relative bandwidth.

However, in all the aforementioned time-frequency transforms, there is a drawback that difficult its practical implementation: they are much more costly, in terms of computing resources and time, than the simple FFT used in MCSA. For example, in the case of the STFT, the FFT must be applied to each one of the windowed signals that result as the time window slides along each one of the current signal samples. This implies to multiply the computation of a single current spectrum by the number of samples of the current, which can be several orders of magnitude in the case of long acquisition times and a high sampling frequency. For example, a 100 s current signal sampled at 100 kHz produces 10^7 samples, so that a full STFT representation of the current would need to compute 10^7 different FFTs.

Is it possible to perform the analysis of the current in transient regime, using either a constant or a relative bandwidth analysis, with the cost of a single FFT? The answer to this question, presented in this paper, is affirmative, and relies on the use of the discrete harmonic wavelet transform (DHWT).

The DHWT is a member of the family of discrete wavelet transforms (DWT), which are being used extensively for the diagnosis of rotating machinery in the time-frequency domain [1], [8]–[11], for the diagnosis of power system disturbances [12]–[16], for the diagnosis of mechanical parts and structures [17]–[19], or even for the development of biosensors [20] and electronic sensors [21]. However, the implementation of a diagnostic system based on the DWT of the motor current faces practical problems, which have been extensively pointed out in the technical literature:

- The frequency bands of the DWT are fixed, and depend only on the sampling frequency. Choosing the correct sampling frequency to isolate the mains component into a given band, for avoiding the leakage over adjacent bands, is crucial to guarantee that the fault signature can be revealed.
- The amplitude of the fault components is very small compared with the mains amplitude, so a slight leakage in the frequency band that contains the mains component, due to the non-ideal behaviour of the DWT filters, may hide the fault harmonics in the adjacent bands. This problem depends on the election of the mother wavelet (Bior [9], Mexican [18], Daubechies [19], [20], etc) and the tuning of their parameters (Daubechies-44, Daubechies-10, etc.), which define the shape of the high-pass and low-pass filters used in the wavelet analysis.
- Although the DWT is very fast, compared with continuous time-frequency transforms, the computation of the filters needed to implement a given DWT analysis is costly, because they differ greatly on the frequency band that they span and on the number of coefficients needed to implement them.

The method proposed in the paper solves these problems:

- The DHWT allows the maximum flexibility in the selection of the frequency bands of the DWT decomposition. In this way a very narrow band can be used to isolate the mains component, leaving the rest of the bands available for displaying the fault signature.
- The DHWT uses ideal frequency filters, so the leakage of the mains component into adjacent frequency bands is very small, allowing the use of these bands for displaying the fault signature.
- The computation cost of the proposed approach is very low: just one FFT and as many IFFTs as desired frequency bands are needed. And there are extremely efficient FFT algorithms, which are available even for embedded devices. This feature allows implementing the proposed method using online diagnostic devices such as DSPs or FPGAs.

So, the proposed approach represents an improvement of the DWT techniques available for performing the diagnosis of the induction motor through the currents in transient regime, obtained through the use of a particular implementation of the mother wavelet. Up to the best knowledge of the authors, this improvement has not been proposed before in this field, in spite of its great advantages from a practical point of view.

The structure of the paper is the following one. In Section II, the fault diagnosis of rotating electrical machines using the DWT of the machine's current is reviewed. In Section III, the proposed diagnostic method, based on the use of the DHWT, is presented, and it is validated in Section IV with the diagnosis of a large 3.15 MW motor with a broken bar during the start-up transient. Finally, Section V presents the conclusions of the work.

II. Fault Diagnosis of Rotating Electrical Machines using the DWT

The proposed method is a particular implementation of the more general DWT-based diagnostic methods, so in this section the use of the DWT for fault diagnosis of rotating electrical machines is reviewed.

The DWT of the motor current has been used extensively for detecting, in transient regime, faults such as eccentricity [1], stator faults [7], broken bars [22]–[24], rotor asymmetries [10], [11], and short circuit faults [25], among others types of faults. As stated in [26], this diagnostic technique is a four-step process that involves:

- Sampling of the transient motor current, with a sampling frequency f_{s}, during an acquisition time T_{acq}.
- Computation of the wavelet transform of the current signal, after a proper selection of the mother wavelet and the number of decomposition levels.
- Analysis of the wavelet coefficients.
- Diagnostic conclusion.

The proposed DHWT approach greatly simplifies the second step of the general DWT-based diagnostic procedure, using just the FFT as the signal processing tool, as will be shown in the following sections.

The first step in the DWT-based diagnostic process is the uniform sampling of the current signal $i(t)$, giving a discrete sequence $\mathbf{i}[n]$, $n = 1 \dots N$, with $N = T_{\mathrm{acq}} \times f_{\mathrm{s}}$. The DWT

performs the decomposition of $\mathbf{i}[n]$, into an approximation signal at a certain decomposition level k, $\mathbf{A}_{\mathrm{k}}[n]$, and k detail signals $\mathbf{D}_{\mathrm{j}}[n]$, $j = 1 \ldots k$,

$$\mathbf{i}[n] = \mathbf{A}_{\mathrm{k}}[n] + \sum_{j=1}^{k} \mathbf{D}_{\mathrm{j}}[n] = \sum_{i=1}^{\frac{N}{2k}} a_{\mathrm{i}}^{\mathrm{k}} \mathbf{\Phi}_{\mathrm{i}}^{\mathrm{k}}[n] + \sum_{j=1}^{k} \sum_{i=1}^{\frac{N}{2j}} d_{\mathrm{i}}^{\mathrm{j}} \mathbf{\Psi}_{\mathrm{i}}^{\mathrm{j}}[n], \tag{1}$$

where $\mathbf{\Phi}^{\mathrm{k}}$ and $\mathbf{\Psi}^{\mathrm{j}}$ are, respectively, the scaling function at level k and the wavelet function at level j. The DWT coefficients $a_{\mathrm{i}}^{\mathrm{k}}$ and $d_{\mathrm{i}}^{\mathrm{j}}$ in (1) are computed using a subband coding algorithm. It has been represented in Fig. 1 and Fig. 2, applied to a current signal sampled at frequency f_{s}, for $k = 2$.

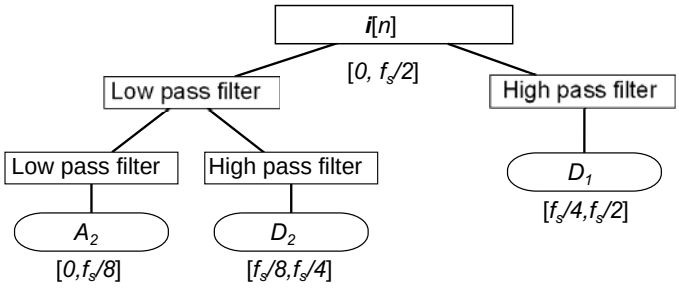

Fig. 1. DWT coefficients computed with a subband coding algorithm, for a number of levels k=2.

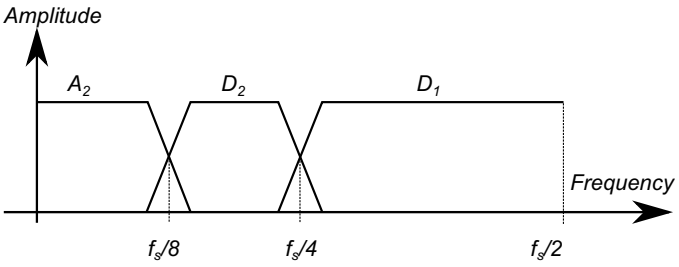

Fig. 2. Filter bank used in the DWT, for a number of levels k=2.

The response of the DWT filter bank to an impulse signal, using a Daubechies-44 (db44) mother wavelet, is shown in Fig. 3, where the multi-resolution property of the DWT can be observed: the low frequency signal components are captured with a high frequency resolution $(0 - f_{\mathrm{s}}/8)$, and the high frequency components are resolved with a fine temporal resolution.

Nevertheless, there is a drawback related to the practical implementation of the DWT-based diagnostic process: the frequency bands covered by the DWT decomposition overlap, due to the non-ideal frequency behaviour of the DWT filters, as shown in Fig. 2. The magnitude response of the high pass and the low pass filters in the case of a widely used mother wavelet, the Daubechies 44, are shown in Fig. 4. From a practical point of view, this overlapping implies that the energy of signal's components whose frequencies are close to the border of a given frequency band can leakage into the neighbouring bands, appearing as false harmonics components. This affects especially to the mains component, whose amplitude can be very high compared to the fault harmonics: the mains leakage in this case can completely hide the small fault components in

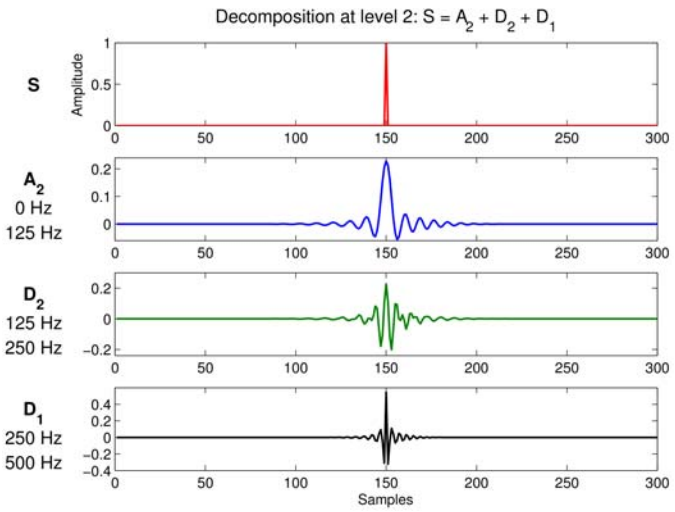

Fig. 3. DWT at level $k = 2$ of a pulse signal using a Daubechies-44 mother wavelet.

the adjacent bands. To solve this problem, widely reported in the technical literature, it is necessary to select a sampling frequency f_{s} that centers one of the DWT bands on the mains frequency, using the expression for the frequency band spanned by a detail signal at a given level j,

$$f(D_j) \in [\frac{f_{\mathrm{s}}}{2^{j+1}}, \frac{f_{\mathrm{s}}}{2^j}]. \tag{2}$$

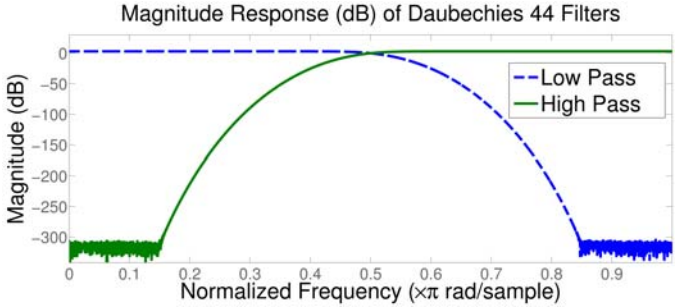

Fig. 4. Magnitude responses of the high pass and low pass filters of a Daubechies-44 mother wavelet.

For example, in the case of $f_{\mathrm{mains}} = 50$ Hz, using a sampling frequency of 5000 samples/s would give a detail signal of level 6 whose frequency band spans

$$f(D_6) \in [\frac{5000}{2^7}, \frac{5000}{2^6}] = [39.0625 \text{ Hz}, 78.125 \text{ Hz}], \tag{3}$$

centered on the mains frequency.

The problem of using non-ideal filters also arises in a variant of the DWT, the discrete wavelet packet transform (DWPT), which uses the same decomposition tree of the DWT of Fig. 1, but performs a full decomposition of both the approximation signal and the detail signal at each level of the tree, as in [14]. The k-level DWPT of the current signal, sampled at f_{s} samples/s, is a high resolution decomposition in frequency bands with a constant bandwidth

$$f_{band} = \frac{f_{\mathrm{s}}}{2^{k+1}}, \tag{4}$$

as shown in Fig. 5 and in Fig. 6.

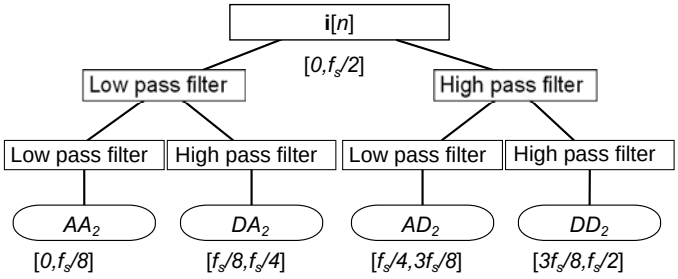

Fig. 5. DWPT coefficients computed with a subband coding algorithm, for a number of levels k=2.

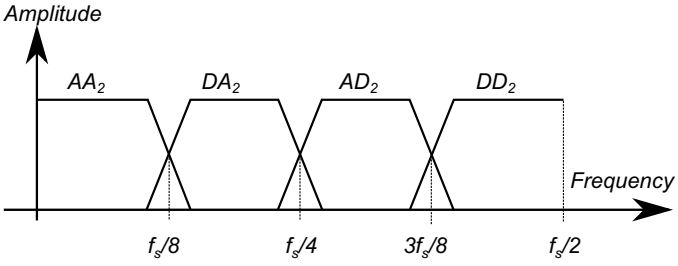

Fig. 6. Filter bank used in the DWPT, for a number of levels k=2.

III. Fault Diagnosis of Rotating Electrical Machines with the Proposed Method, using the DHWT

The proposed approach, based entirely on the use of the FFT, and its inverse, the IFFT, relies on the election of a particular scaling function, the sinc function,

$$\phi(t) = \frac{\sin(\pi t)}{\pi t}, \tag{5}$$

and its associated mother wavelet, the harmonic wavelet

$$\psi(t) = \frac{\sin(\pi t/2)}{\pi t/2}\cos(3\pi t/2). \tag{6}$$

The particularity of these functions is that the low pass and high pass filters that they generate are ideal ones, that is, their frequency responses do not overlap, as shown in Fig. 7.

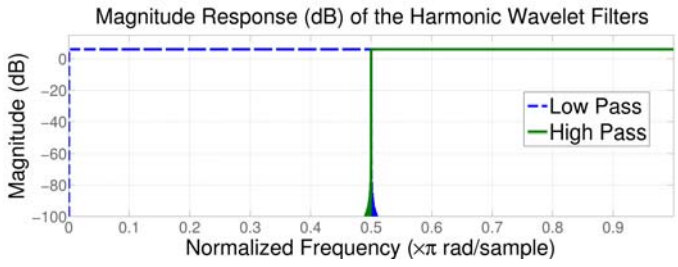

Fig. 7. Magnitude responses of the high pass and low pass filters of a harmonic mother wavelet.

The multi-resolution filter bank used to implement the DHWT with the filters depicted in Fig. 7, is shown in Fig. 8. Due to the ideal behaviour of the DHWT filters, this filter bank can be implemented very effectively in the frequency domain, by spectral windowing, instead of applying the filters in the time domain. The process needed to perform the DHWT of the motor current is very simple, and reduces to (Fig. 9):

- Capturing the transient motor current.
- Obtaining the complex spectrum of the current signal (modulus and argument), using the FFT.
- Applying a rectangular window to the current's spectrum, equal to one within the frequency band spanned by each desired wavelet component (2), and zero elsewhere.
- Transferring each windowed spectrum back to the time domain with the IFFT, which generates the desired approximation and detail components of the transient current signal.

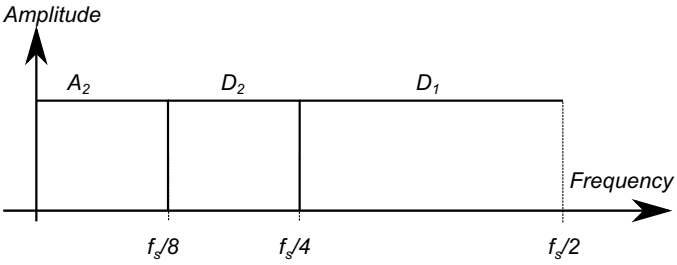

Fig. 8. Filter bank used in the DHWT, for a number of levels k=2.

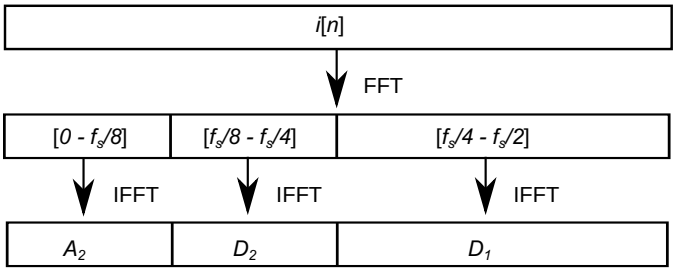

Fig. 9. DHWT at level $k = 2$ of the current signal, using the proposed FFT-based approach to implement the filter bank of Fig. 8.

It is an extended assumption that the Fourier transform (FT) cannot be applied to the analysis of transient currents, because the power spectrum only gives the magnitude of the current harmonics, but not their time localization. On the contrary, the complex spectrum of a transient signal preserves its time-related characteristics. For example, the FT of a Dirac-delta impulse located at the time origin is just a constant unit real value,

$$\delta(t) \quad \xrightarrow{\text{FT}} \quad \hat{\delta}(f) = 1 \times e^{j0}. \tag{7}$$

If the pulse is shifted to a time t_0, the modulus of its FT has still a constant unit value, but the time shift generates a linear shift of the spectrum phase

$$\delta(t - t_0) \quad \xrightarrow{\text{FT}} \quad \hat{\delta}(f) = 1 \times e^{-j2\pi f t_0}. \tag{8}$$

As (8) states, the complex spectrum of a transient signal contains the information needed to locate its components precisely in the time domain, which allows the proposed DHWT approach. Fig. 10 shows the DHWT of an isolated pulse signal, using the frequency bands depicted in Fig. 9.

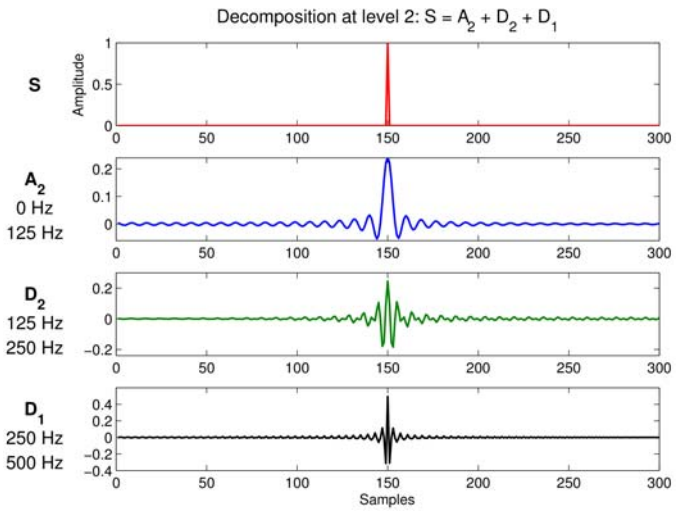

Fig. 10. DHWT at level $k = 2$ of a pulse signal, using the proposed FFT-based approach.

The results obtained show that the DHWT, although being based entirely on the FFT, can locate precisely a transient signal in the time domain. Besides, the impulse responses shown in Fig. 10 give the scaling (5) and the wavelet (6) functions of the DHWT for each frequency band. Nevertheless, the ideal filters in the frequency domain used by the DHWT (Fig. 8), cannot be ideal also in the time domain, due to the Heisenberg principle, and they have wider time side-lobes than the non-ideal Daubechies filters shown in Fig. 2. This causes a higher ripple in the time components of the Dirac pulse extracted by the DHWT (Fig. 10) compared with the time components generated by the DWT (Fig. 3), and this constitutes a trade-off of the use of ideal frequency filters. Nevertheless, the ripple effect, which appears always when filtering sharp signals, is greatly reduced when analysing the motor current, which is a smooth signal.

The same method used to implement the DHWT can be used also to perform the discrete harmonic wavelet packet transform (DHWPT) of the motor current. The only difference with the DHWT is the length of the rectangular windows that are applied to the current's spectrum: instead of using frequency-dependent window lengths, as in Fig. 8, the DHWPT uses constant-length spectral windows, as in Fig. 11. The proposed FFT implementation of the DHWPT is shown in Fig. 12.

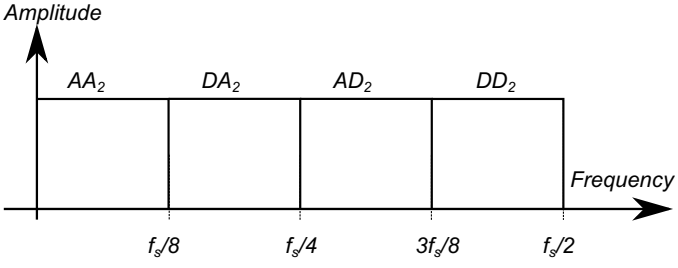

Fig. 11. Filter bank used in the DHWPT, for a number of levels k=2.

The sinc scaling function, (5), and the harmonic wavelet, (6), have been used previously in the analysis of vibrations

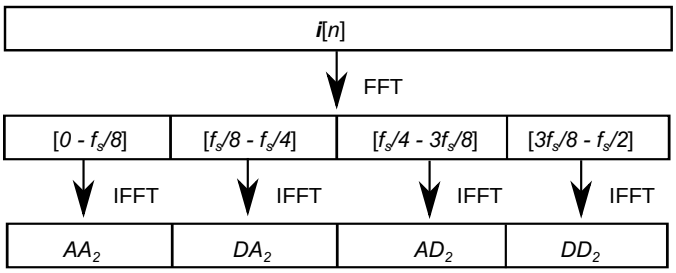

Fig. 12. DHWPT at level $k = 2$ of the current signal, using the proposed FFT-based approach to implement the filter bank of Fig. 11.

by [27]–[32]. They are also known in the signal processing literature as Littlewood-Palley wavelets [33], and Shannon wavelets. However, up to the best of the authors' knowledge, these types of wavelets have not yet been used in a diagnostic process based on the analysis of the machine current in transient conditions, in spite of its advantages in terms of computational simplicity and ideal filtering performance.

IV. Validation of the Proposed Approach

To validate the proposed approach, in this section it is applied to the detection of a broken bar fault during the start-up transient of a squirrel cage induction motor. This election is not exclusive, because other fault types and working regimes, which have been analysed in the technical literature using the DWT, can also be effectively detected using the proposed DHWT method.

The validation is performed in two stages. First, in Section IV-A, the characteristic pattern that a motor with broken bars generates in the time-frequency domain during the start-up transient is described using the DHWT and the DHWPT. Second, in Section IV-B, this pattern is identified with the proposed approach in the case of a large 3.15 Mw industrial motor with a broken bar, and the results are compared with the DWT and the DWPT of the motor current using a db44 mother wavelet.

A. Analysis of the Current of an Induction Motor with a Broken Bar During the Startup Transient, Using the DHWT

The diagnosis of the broken bar fault during the start-up transient can be performed by detecting the evolution in the time-frequency domain of the lower sideband harmonic (LSH), generated by this type of fault. The frequency of the LSH varies with the slip s of the machine as

$$f_{LSH}(s) = (1 - 2s) f_{\text{mains}}, \tag{9}$$

where f_{mains} is the supply's frequency.

The LSH of a simulated induction motor, sampled at 5 kHz, has been computed and presented in [34], and it is shown in Fig. 13.

From (9), during the start-up transient, the frequency of the LSH continuously decreases from the supply's frequency when the machine is connected ($t = 0$), and it becomes null when the rotor speed equals half the synchronous speed, $s = 0.5$ in (9). From this point, the frequency of the LSH

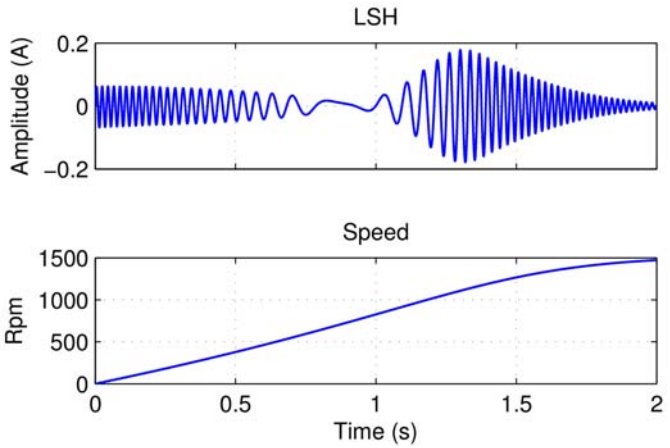

Fig. 13. Lower sideband harmonic of a simulated induction motor with a broken bar during the start-up transient. Top: amplitude of the LSH. Bottom: speed during the transient.

increases again, reaching a constant value in stationary regime. This V-shaped pattern in the time-frequency domain during a start-up transient constitutes a characteristic signature of the broken bar fault, and has been used for diagnostic purposes in [34] and [26]. This signature can be revealed by applying the proposed DHWT to the LSH depicted in Fig. 13, as shown in Fig. 14. Besides, the proposed approach allows choosing the dyadic structure of the wavelet tree that is best suited to the signal under analysis, independently from the supply's frequency, without the constraint of (2).

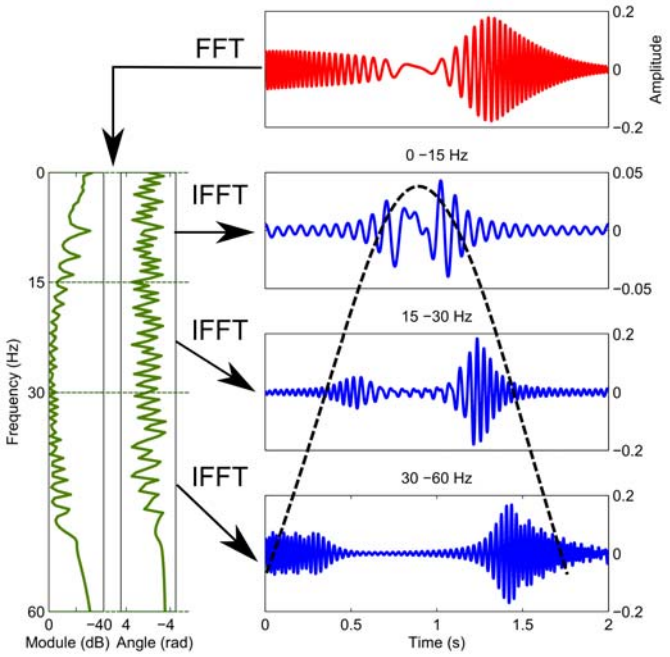

Fig. 14. DHWT of the LSH during the start-up transient of an induction motor with a broken bar.

The LSH signal of Fig. 13 has been analysed also with the proposed DHWPT approach, splitting the spectrum of the LSH in frequency bands with a constant bandwidth of 9 Hz, and performing the IFFT of each band. The result, shown in Fig. 15, displays clearly its characteristic pattern in the time-frequency domain during the start-up transient of the motor.

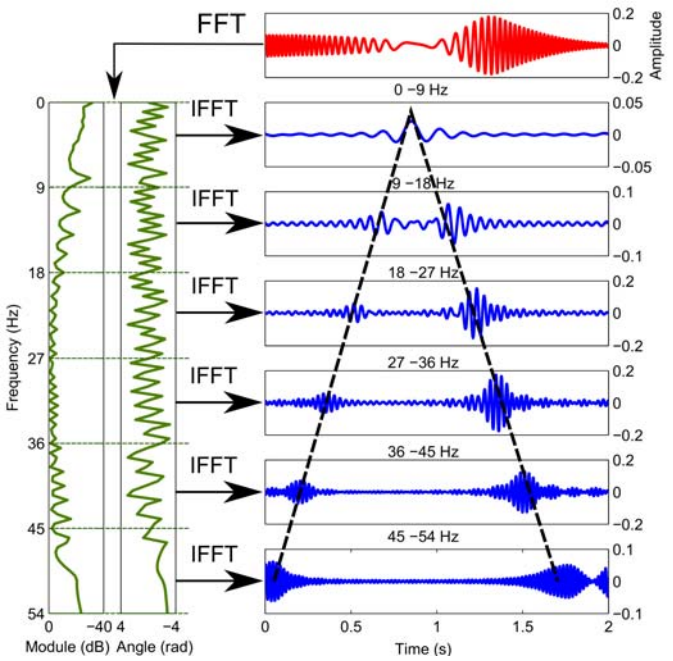

Fig. 15. DHWPT of the LSH during the start-up transient of an induction motor with a broken bar.

B. Fault Diagnosis of a 3.15 MW Motor With a Broken Bar During the Startup Transient, Comparing the Proposed DHWT Approach and the DWT Results

A 3.15 MW, grid-connected, high-voltage induction motor, which drives a low and a high-pressure pumps in a thermal power plant-heating plant, shown in Fig. 16, has been analysed using the proposed method, and a broken bar fault has been detected. A visual inspection revealed that, in fact, the motor had one broken bar, as shown in Fig. 17.

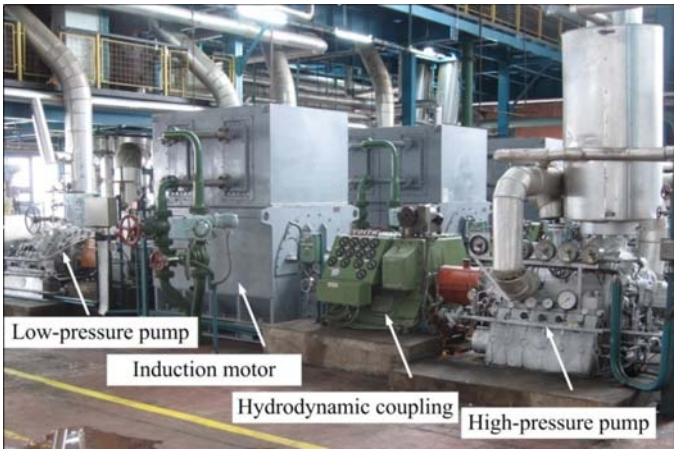

Fig. 16. The 3.15 MW motor used for validating the proposed method, installed in the thermal power plant-heating plant.

The proposed method has been applied to the motor start-up current, sampled at 5 kHz, in order to detect the characteristic

Fig. 17. Broken bar of the 3.15 MW motor used for the experimental validation of the proposed method.

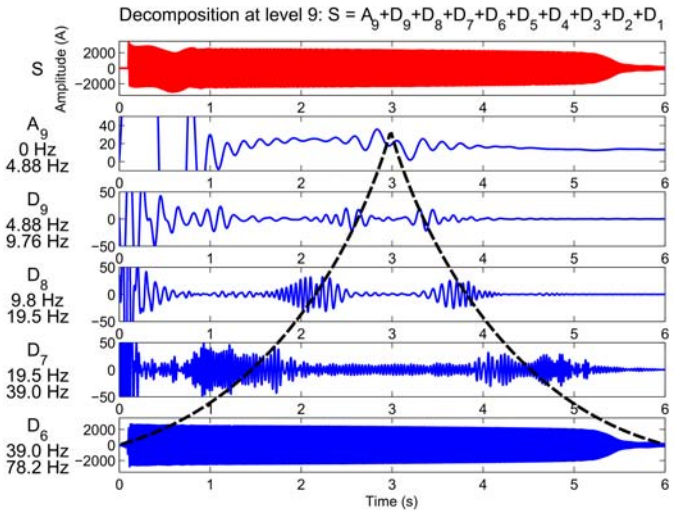

Fig. 18. DWT at level $k = 9$, with a Daubechies 44 mother wavelet, of the start-up current of the 3.15 MW motor with a broken bar. The dashed line highlights the evolution of the LSH during the start-up transient.

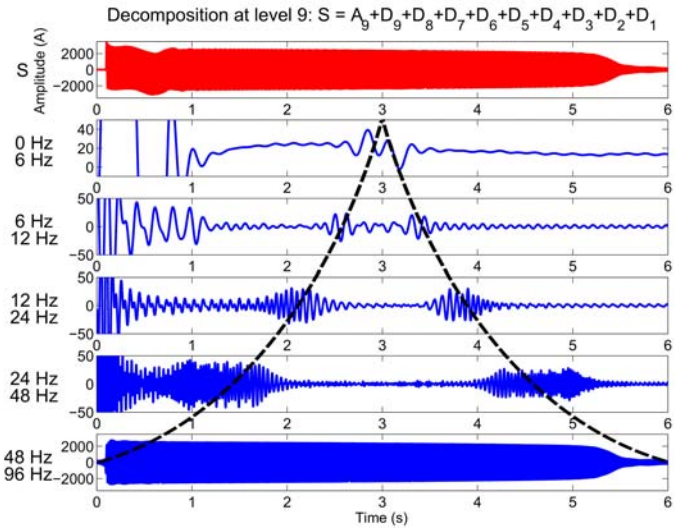

Fig. 19. Proposed DHWT at level $k = 9$ of the start-up current of the 3.15 MW motor with a broken bar. The dashed line highlights the evolution of the LSH during the start-up transient.

pattern of the LSH in the time-frequency domain. To validate the proposed method, the results are compared with those obtained with a classical db44 DWT of the current motor.

The analysis of the motor current during the start-up transient has been performed first with a 9-level DWT, using a db44 mother wavelet, as in [26]. As indicated in (3), the detail signal of level 6 ($[39\text{ Hz} - 78\text{ Hz}]$) contains the mains component, so that three additional detail signals plus the approximation signal can be used to track the evolution of the LSH (see Fig. 18). In this case, the position of the frequency bands depend on the sampling frequency (2), and the frequency range available for detecting the LSH signature is limitied to the [0 - 39 Hz]. Besides, any change in the value of the sampling frequency would change the limits of the frequency bands.

The analysis of the same motor current has been performed using the proposed FFT-based DHWT approach, that is, applying a rectangular window (with a frequency dependent length) to the current's complex spectrum, transforming the windowed spectrum back to the time domain, and repeating the process for each desired frequency band (see Fig. 19). In this case the position of the frequency bands does not depend on the sampling frequency

As it can be observed in Fig. 18 and Fig. 19, the proposed DHWT method can detect the fault through the evolution of the LSH, as in the case of a classical db44 DWT, but using just a single FFT of the current signal instead of using a multi-resolution time-domain filter bank. Besides, with the proposed approach, the position of the frequency bands can be chosen independently from the sampling frequency. And, due to the ideal behaviour of the DHWT filters, the frequency range available for detecting the LSH signature can be extended near the mains frequency. Comparing the proposed approach in Fig. 19 with the traditional DWT shown in Fig. 18, the range has been extended from [0- 39 Hz] up to [0- 48 Hz].

A second analysis of the start-up current of the faulty motor has been performed with the DWPT, that is, with approximation and detail signals of constant bandwidth. The DWPT of the motor current using a db44 mother wavelet, with 8 levels of decomposition, is shown in Fig. 20. Due to the small bandwidth of the filters (9.77 Hz), and to the overlapping in the frequency domain of adjacent db44 filters (see Fig. 6), the energy of the mains component, (50 Hz) leaks into the adjacent band ($[39.1\text{ Hz} - 48.8\text{ Hz}]$), and makes this band unavailable for detecting the LSH.

The analysis of the same motor current has been performed using the proposed FFT-based DHWPT approach, that is, applying a rectangular window (with a constant length) to the current's complex spectrum, transforming the windowed spectrum back to the time domain, and repeating the process for each desired frequency band (see Fig. 21).

In the case of the proposed DHWPT approach, besides obtaining a better spectral behaviour due to the use of the harmonic wavelet filters, there is an additional advantage: it is not necessary to use filters whose bandwidth depend on the sampling frequency, as constrained by (4). Instead, the analysis

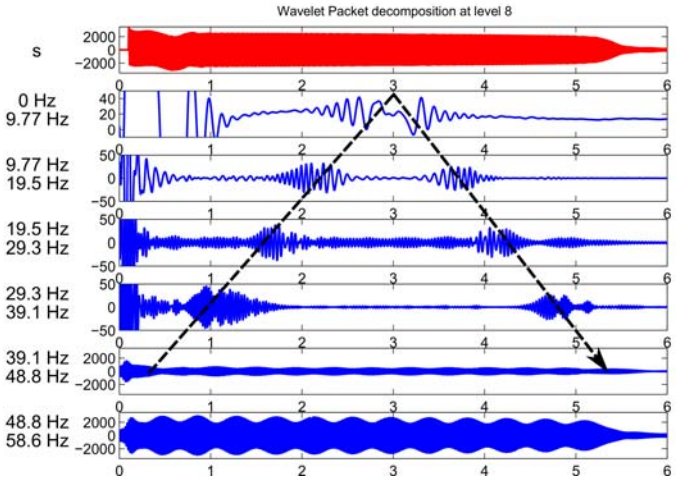

Fig. 20. DWPT at level $k = 8$, with a Daubechies 44 mother wavelet, of the start-up current of the 3.15 MW motor with a broken bar. The dashed line highlights the evolution of the LSH during the start-up transient.

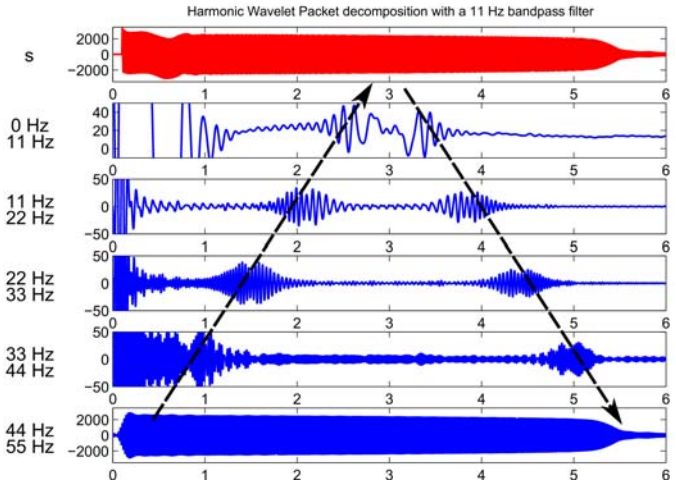

Fig. 21. Proposed DHWPT at level $k = 8$ of the start-up current of the 3.15 MW motor with a broken bar. The dashed line highlights the evolution of the LSH during the start-up transient.

with the proposed method has been performed using a constant rectangular window in the frequency domain with a bandwidth of 11 Hz, which isolates and centers the mains component in a $[44\ \text{Hz} - 55\ \text{Hz}]$ band, eliminating any leakage into adjacent bands. In this way, a better picture of the evolution of the LSH is obtained with the proposed approach in Fig. 21, compared with the results obtained with a db44 DWPT in Fig. 20. This freedom of election of the frequency bands is not possible using the classical DWPT, where it is strictly imposed by the sampling frequency and the number of decomposition levels (2). Moreover, the proposed method is not only very simple to implement, but also very fast to compute. The time needed to compute the db44 wavelet packet transform is of 1.25 seconds, while the computation of the proposed harmonic packet transform is made in just 0.58 seconds, using the same computer.

As a remark about the flexibility of the proposed method, the start-up current of the 3.15 MW motor has been analysed also by slicing its FFT transform in two adjacent frequency bands with very different frequency bandwidths (Fig. 22):

- A low frequency band, with a wide bandwidth ($[0\ \text{Hz} - 47\ \text{Hz}]$), which contains the LSH.
- A high frequency band, with a narrow bandwidth ($[47\ \text{Hz} - 53\ \text{Hz}]$), which encloses the mains component.

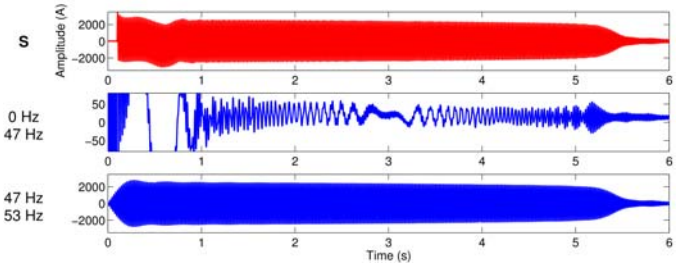

Fig. 22. Extraction of the LSH from the start-up current of the 3.15 MW motor with a broken bar, using a low frequency band with a wide bandwidth to extract the LSH, and a high frequency band, with a narrow bandwidth, to isolate the mains component.

The results of this decomposition, Fig. 22, show that the LSH can be extracted cleanly and very precisely from the start-up current using these customized frequency bands. In fact, the experimental LSH of Fig. 22 follows an evolution with a shape very similar to the shape predicted in Fig. 13.

V. Conclusions

In this work, the FFT- based discrete harmonic wavelet. has been proposed as a valid tool for the diagnosis of electrical machines working in transient conditions. It is a common assumption to consider that the FFT can only be applied to the diagnosis of electrical machines working in steady state, because the power spectrum is not able to locate in the time domain the signal components. However, using the complex spectrum of the current, a new diagnostic method has been developed in this paper, which performs the fault diagnosis of rotating electrical machines in transient conditions using just the FFT of the current (and its inverse, the IFFT). This fact makes the proposed approach very fast and very easy to implement. Besides, the proposed method allows selecting freely the frequency bands used in the current decomposition, independently of the sampling frequency or the number of decomposition levels. This feature opens new possibilities for adapting the frequency bands to the working conditions of the machine or the type of fault to be detected, in order to capture better the transient behaviour of the fault harmonics, or to measure more precisely their energy content. Moreover, the flexibility of the proposed DHWT decomposition makes it possible to detect the fault harmonic signature in cases where the traditional DWT approach may fail. For example, in the case of noise sources with fixed frequencies in the range spanned by the transient fault components, the DHWT can easily eliminate narrow frequency bands containing the noise signals, which cannot be done with a traditional DWT approach.

The wide availability of the FFT in modern software and control devices, and the simplicity and speed of the

proposed approach, makes it especially well suited for its implementation on embedded devices, such as FPGAs and DSPs.

APPENDIX

Motor characteristics: three-phase induction motor, star connection. Rated characteristics: $P = 3150$ kW, $f = 50$ Hz, $U = 6$ kV, $I = 373$ A , $n = 2982$ rpm, $\cos\varphi = 0.92$, number of bars = 56.

REFERENCES

[1] K. Yahia, A. Cardoso, A. Ghoggal, and S. Zouzou, "Induction motors airgap-eccentricity detection through the discrete wavelet transform of the apparent power signal under non-stationary operating conditions," *ISA Transactions*, vol. 53, no. 2, pp. 603 – 611, 2014.

[2] Y. Gritli, S. B. Lee, F. Filippetti, and L. Zarri, "Advanced Diagnosis of Outer Cage Damage in Double-Squirrel-Cage Induction Motors Under Time-Varying Conditions Based on Wavelet Analysis," *Industry Applications, IEEE Transactions on*, vol. 50, no. 3, pp. 1791–1800, May 2014.

[3] E. Strangas, S. Aviyente, and S. Zaidi, "Time-Frequency Analysis for Efficient Fault Diagnosis and Failure Prognosis for Interior Permanent-Magnet AC Motors," *Industrial Electronics, IEEE Transactions on*, vol. 55, pp. 4191–4199, Dec. 2008.

[4] Y. Yang, W. Zhang, Z. Peng, and G. Meng, "Multicomponent Signal Analysis Based on Polynomial Chirplet Transform," *Industrial Electronics, IEEE Transactions on*, vol. 60, pp. 3948–3956, Sept. 2013.

[5] S. Nandi, T. Ilamparithi, S.-B. Lee, and D. Hyun, "Detection of Eccentricity Faults in Induction Machines Based on Nameplate Parameters," *Industrial Electronics, IEEE Transactions on*, vol. 58, pp. 1673–1683, May 2011.

[6] M. Riera-Guasp, M. Pineda-Sanchez, J. Perez-Cruz, R. Puche-Panadero, J. Roger-Folch, and J. Antonino-Daviu, "Diagnosis of Induction Motor Faults via Gabor Analysis of the Current in Transient Regime," *Instrumentation and Measurement, IEEE Transactions on*, vol. 61, pp. 1583–1596, June 2012.

[7] J. Seshadrinath, B. Singh, and B. Panigrahi, "Investigation of Vibration Signatures for Multiple Fault Diagnosis in Variable Frequency Drives Using Complex Wavelets," *Power Electronics, IEEE Transactions on*, vol. 29, pp. 936–945, Feb. 2014.

[8] J. Wang, Q. He, and F. Kong, "Adaptive multiscale noise tuning stochastic resonance for health diagnosis of rolling element bearings," *Instrumentation and Measurement, IEEE Transactions on*, vol. 64, no. 2, pp. 564–577, Feb 2015.

[9] I. Bediaga, X. Mendizabal, I. Etxaniz, and J. Munoa, "An Integrated System for Machine Tool Spindle Head Ball Bearing Fault Detection and Diagnosis," *Instrumentation Measurement Magazine, IEEE*, vol. 16, no. 2, pp. 42–47, April 2013.

[10] Y. Gritli, L. Zarri, C. Rossi, F. Filippetti, G. Capolino, and D. Casadei, "Advanced Diagnosis of Electrical Faults in Wound-Rotor Induction Machines," *Industrial Electronics, IEEE Transactions on*, vol. 60, pp. 4012–4024, Sept. 2013.

[11] F. Vedreno-Santos, M. Riera-Guasp, H. Henao, M. Pineda-Sanchez, and R. Puche-Panadero, "Diagnosis of Rotor and Stator Asymmetries in Wound-Rotor Induction Machines Under Nonstationary Operation Through the Instantaneous Frequency," *Industrial Electronics, IEEE Transactions on*, vol. 61, no. 9, pp. 4947–4959, Sept 2014.

[12] M. Manikandan, S. Samantaray, and I. Kamwa, "Detection and Classification of Power Quality Disturbances Using Sparse Signal Decomposition on Hybrid Dictionaries," *Instrumentation and Measurement, IEEE Transactions on*, vol. 64, no. 1, pp. 27–38, Jan 2015.

[13] W. Li, A. Monti, and F. Ponci, "Fault Detection and Classification in Medium Voltage DC Shipboard Power Systems With Wavelets and Artificial Neural Networks," *Instrumentation and Measurement, IEEE Transactions on*, vol. 63, no. 11, pp. 2651–2665, Nov 2014.

[14] J. Barros, R. Diego, and M. de Apraz, "A Discussion of New Requirements for Measurement of Harmonic Distortion in Modern Power Supply Systems," *Instrumentation and Measurement, IEEE Transactions on*, vol. 62, no. 8, pp. 2129–2139, Aug 2013.

[15] F. Bezerra Costa, "Fault-Induced Transient Detection Based on Real-Time Analysis of the Wavelet Coefficient Energy," *Power Delivery, IEEE Transactions on*, vol. 29, pp. 140–153, Feb. 2014.

[16] S. Jain and S. Singh, "Fast Harmonic Estimation of Stationary and Time-Varying Signals Using EA-AWNN," *Instrumentation and Measurement, IEEE Transactions on*, vol. 62, no. 2, pp. 335–343, Feb 2013.

[17] L. Rosado, F. Janeiro, P. Ramos, and M. Piedade, "Defect Characterization With Eddy Current Testing Using Nonlinear-Regression Feature Extraction and Artificial Neural Networks," *Instrumentation and Measurement, IEEE Transactions on*, vol. 62, no. 5, pp. 1207–1214, May 2013.

[18] H. Hosseinabadi, B. Nazari, R. Amirfattahi, H. Mirdamadi, and A. Sadri, "Wavelet Network Approach for Structural Damage Identification Using Guided Ultrasonic Waves," *Instrumentation and Measurement, IEEE Transactions on*, vol. 63, no. 7, pp. 1680–1692, July 2014.

[19] D. Sun, Y. Yan, R. Carter, L. Gao, G. Lu, G. Riley, and M. Wood, "On-Line Nonintrusive Detection of Wood Pellets in Pneumatic Conveying Pipelines Using Vibration and Acoustic Sensors," *Instrumentation and Measurement, IEEE Transactions on*, vol. 63, no. 5, pp. 993–1001, May 2014.

[20] K. Luo, J. Li, and J. Wu, "A Dynamic Compression Scheme for Energy-Efficient Real-Time Wireless Electrocardiogram Biosensors," *Instrumentation and Measurement, IEEE Transactions on*, vol. 63, no. 9, pp. 2160–2169, Sept 2014.

[21] P. Saha, S. Ghorai, B. Tudu, R. Bandyopadhyay, and N. Bhattacharyya, "A Novel Technique of Black Tea Quality Prediction Using Electronic Tongue Signals," *Instrumentation and Measurement, IEEE Transactions on*, vol. 63, no. 10, pp. 2472–2479, Oct 2014.

[22] A. Ordaz-Moreno, R. de Jesus Romero-Troncoso, J. Vite-Frias, J. Rivera-Gillen, and A. Garcia-Perez, "Automatic Online Diagnosis Algorithm for Broken-Bar Detection on Induction Motors Based on Discrete Wavelet Transform for FPGA Implementation," *Industrial Electronics, IEEE Transactions on*, vol. 55, pp. 2193–2202, May 2008.

[23] A. Bouzida, O. Touhami, R. Ibtiouen, A. Belouchrani, M. Fadel, and A. Rezzoug, "Fault Diagnosis in Industrial Induction Machines Through Discrete Wavelet Transform," *Industrial Electronics, IEEE Transactions on*, vol. 58, pp. 4385–4395, Sept. 2011.

[24] M. Pineda-Sanchez, M. Riera-Guasp, J. Roger-Folch, J. Antonino-Daviu, J. Perez-Cruz, and R. Puche-Panadero, "Diagnosis of Induction Motor Faults in Time-Varying Conditions Using the Polynomial-Phase Transform of the Current," *Industrial Electronics, IEEE Transactions on*, vol. 58, pp. 1428–1439, Apr. 2011.

[25] K. Iyer, X. Lu, Y. Usama, V. Ramakrishnan, and N. Kar, "A Twofold Daubechies-Wavelet-Based Module for Fault Detection and Voltage Regulation in SEIGs for Distributed Wind Power Generation," *Industrial Electronics, IEEE Transactions on*, vol. 60, pp. 1638–1651, Apr. 2013.

[26] M. Riera-Guasp, J. Antonino-Daviu, M. Pineda-Sanchez, R. Puche-Panadero, and J. Perez-Cruz, "A General Approach for the Transient Detection of Slip-Dependent Fault Components Based on the Discrete Wavelet Transform," *Industrial Electronics, IEEE Transactions on*, vol. 55, pp. 4167–4180, Dec. 2008.

[27] D. E. Newland, "Harmonic wavelet analysis," *Proceedings of the Royal Society of London. Series A: Mathematical and Physical Sciences*, vol. 443, no. 1917, pp. 203–225, 1993.

[28] ——, "Harmonic wavelets in vibrations and acoustics," *Philosophical Transactions of the Royal Society of London. Series A: Mathematical, Physical and Engineering Sciences*, vol. 357, no. 1760, pp. 2607–2625, 1999.

[29] D. Newland, "Ridge and phase identification in the frequency analysis of transient signals by harmonic wavelets," *Journal of Vibration and Acoustics*, vol. 121, no. 2, pp. 149–155, 1999.

[30] D. E. Newland, "Time-frequency and time-scale signal analysis by harmonic wavelets," in *Signal Analysis and Prediction*, ser. Applied and Numerical Harmonic Analysis, A. Prochazka, J. Uhlir, Jan, P. Rayner, and N. Kingsbury, Eds. Birkhäuser Boston, 1998, pp. 3–26.

[31] P. Shi, Z. Chen, and Y. Vagapov, "Wavelet transform based broken rotor-bar fault detection and diagnosis performance evaluations," *International Journal of Computer Applications*, vol. 69, no. 14, 2013.

[32] S. Hou, Y. Li, and Z. Wang, "A resonance demodulation method based on harmonic wavelet transform for rolling bearing fault diagnosis," *Structural Health Monitoring*, vol. 9, no. 4, pp. 297–308, 2010.

[33] J. Gilles, G. Tran, and S. Osher, "2d empirical transforms. wavelets, ridgelets, and curvelets revisited," *SIAM Journal on Imaging Sciences*, vol. 7, no. 1, pp. 157–186, 2014.

[34] M. Pineda-Sanchez, M. Riera-Guasp, J. Antonino-Daviu, J. Roger-Folch, J. Perez-Cruz, and R. Puche-Panadero, "Instantaneous Frequency of the Left Sideband Harmonic During the Start-Up Transient: A New Method for Diagnosis of Broken Bars," *Industrial Electronics, IEEE Transactions on*, vol. 56, pp. 4557–4570, Nov. 2009.

Angel Sapena-Baño obtained its M.Sc. degree in Electrical Engineering in 2009 from the Universitat Politecnica de Valencia (Spain). From 2008 he works as a researcher with the Institute for Energy Engineering of Universitat Politecnica de Valencia. His research interests focus on induction motor diagnostics and maintenance based on condition monitoring, numerical modelling of electrical machines, and advanced automation of industrial processes and electrical installations.

Manuel Pineda-Sanchez (M02) received his M.Sc. degree in 1985 and his Ph.D. degree in 2004 from the Universitat Politecnica de Valencia, both in Electrical Engineering. Currently he is an Associate Professor with the Department of Electrical Engineering of the Universitat Politecnica de Valencia. His research interests include electrical machines and drives, induction motor diagnostics, and numerical simulation of electromagnetic fields.

Ruben Puche-Panadero (M09) received his M.Sc. degree in Automatic and Electronic Engineering in 2003, and its Ph.D. degree in Electrical Engineering in 2008, both from the Universitat Politecnica de Valencia. He joined the Universitat Politecnica de Valencia in 2006 and he is currently Associate Professor of Control of Electrical Machines. His research interests focus on induction motor diagnosis, numerical modeling of electrical machines, and advanced automation processes and electrical installations.

Javier Martínez-Román was born in 1965. He received the Ph.D. degree in Electrical Engineering from the Polytechnic University of Valencia, Spain, in 2002. Currently he is Associate Professor with the Universitat Politecnica de Valencia. His primary areas of interest are electrical machines and drives. Dr. Martnez-Romn has participated in various international projects supported by the European Union. He has published several papers on electrical machines in international journals and conference proceedings.

Dragan Matić was born on October 16th, 1978, in Novi Sad, Serbia. He received the B.Sc. degree in Electrical Engineering in 2004, and the M.Sc. and Ph.D. degree in Electrical Engineering in 2008 and 2012, all from the University of Novi Sad, Serbia. Currently, he is Assistant Professor at the Computing and Control Department at the same University. His research interest is in the field of artificial intelligence and its application in control, modeling, fault detection, and engineering design. He is a member of IEEE.